



PCDD/Fs from a large-scale municipal solid waste incinerator under transient operations: Insight formation pathways and optimal reduction strategies

Shijian Xiong, Peng Yaqi, Lu Shengyong^{*}, Ken Chen, Xiaodong Li, Cen Kefa

State Key Laboratory of Clean Energy Utilization, Zhejiang University, Hangzhou, 310027, PR China

ARTICLE INFO

Keywords:

Polychlorinated dibenzo-p-dioxin and dibenzofuran
Formation pathways
Optimal reduction strategies
Incineration
Transient operations

ABSTRACT

Polychlorinated dibenzo-p-dioxin and dibenzofurans (PCDD/Fs) emissions from the transient operation of municipal solid waste incinerators can reach up to 690 ng/Nm³, as measured in this study. To control the extreme emissions to meet the national standard, the formation pathways of PCDD/F were investigated under transient operations (cold start-up, hot start-up, and after start-up) and normal operations. Compared with normal operations, transient operations facilitate the formation of low-chlorinated congeners rather than highly chlorinated congeners. Statistically, for transient operations, strong correlations were found among tetrachlorodibenzo-p-dioxin or tetrachlorodibenzofuran isomers. An abundant carbon matrix is an important carbon source for PCDD formation. Moreover, the comprehensive study revealed that the oxidation of deposited soot is the main source of PCDD/F emissions, relative to de novo synthesis, chlorobenzene-route synthesis, chlorophenol-route synthesis, and chlorination of dibenzo-p-dioxin/dibenzofuran. In addition, the optimal start-up procedure was constructed by analyzing main formation pathways and operating conditions. The relationship between the international toxic quantity (I-TEQ) values (C_{I-TEQ}) and the reaction time can be assigned as $C_{I-TEQ} = 11.72t^{-0.65}$ ($R^2 = 0.97$) for the circulating fluidized bed. The relationship of $C_{I-TEQ} = 4.61t^{-0.59}$ ($R^2 = 0.85$) was also proven on the dataset with a grate furnace. Then, the optimal feeding rate of activated carbon was further proposed by the relationship between the reaction time and I-TEQ, and the semi-empirical equation for PCDD/Fs adsorption. Finally, the PCDD/Fs emissions can be reduced to 0.1 ng I-TEQ/Nm³ under transient operations according to the time since start-up.

1. Introduction

Incineration has been the mainstream strategy for managing municipal solid waste (MSW) in China owing to its multiple advantages, such as excellent volume reduction and energy recovery (Lin et al., 2020). However, polychlorinated dibenzo-p-dioxins and dibenzofurans (PCDD/Fs) are considered to be the most toxic organic pollutants released from MSW incineration. The PCDD/Fs emissions from MSW incinerators (MSWIs) have an evident influence on the ambient air (Huang et al., 2021), presenting as international toxic equivalent quantity (I-TEQ). Nowadays, PCDD/Fs emissions emitted from MSWIs in continuous stable operation are significantly low (<0.1 ng I-TEQ/Nm³) (Qiu et al., 2020; Xiong et al., 2021) because of the strict national standard (0.1 ng I-TEQ/Nm³) and effective reduction technologies (Chang et al., 2009; Lu et al., 2021). However, PCDD/F emissions under

transient operations (start-up, after start-up (after-start), and shut-down) were as high as 250 ng I-TEQ/Nm³ which markedly exceeds the national standard (Neuer Etscheidt et al., 2006), and has not been included in the emission inventories (Li et al., 2017; Lin et al., 2014). Despite transient operations occurring once/twice per year for maintenance in most MSWI, PCDD/Fs emissions during transient operations are approximately two orders of magnitude higher than those during normal operation (temperature of incinerator outlet is higher than 850 °C, after start-up for more than 1 month). Moreover, the PCDD/Fs emissions under transient operations can be up to two-thirds of the annual PCDD/Fs emissions from MSWIs (Grosso et al., 2007; Neuer Etscheidt et al., 2006). Therefore, PCDD/Fs emissions under transient operations have been recognized as an important source of PCDD/Fs emissions from MSWIs, in which is a concern for researchers, governments, and industrial managers.

To determine the effect of transient operations on PCDD/Fs,

^{*} Corresponding author.

E-mail address: lushy@zju.edu.cn (L. Shengyong).

<https://doi.org/10.1016/j.jenvman.2022.114878>

Received 26 October 2021; Received in revised form 26 February 2022; Accepted 7 March 2022

Available online 18 April 2022

0301-4797/© 2022 Published by Elsevier Ltd.

Nomenclature	
AC	activated carbon
ACI	activated carbon injection
APCDs	air pollution control devices
CBzs	chlorobenzenes
CFB	circulating fluidized bed
CP	chlorophenol
C_{I-TEQ}	I-TEQ concentrations (ng I-TEQ/Nm ³)
d_c	degree of chlorination
DD	dibenzo-p-dioxin
DF	dibenzofuran
EPA	environment protect agency
f	weight percentage of PCDD, PCDF, or PCDD/F congeners (wt. %)
F	AC feeding rate (mg/Nm ³)
F/R	AC feeding concentration
FF	fabric filter
HpCDD	heptachlorodibenzo-p-dioxin
HpCDF	heptachlorodibenzofuran
HxCDD	hexachlorodibenzo-p-dioxin
HxCDF	hexachlorodibenzofuran
k	reaction constants
I-TEQ	international toxic equivalents
OCDD	octachlorodibenzodioxin
OCDF	octachlorodibenzofuran
PAHs	polycyclic aromatic hydrocarbon
PCDD	polychlorinated dibenzo-p-dioxin
PCDF	polychlorinated dibenzofuran
PCDD/Fs	polychlorinated dibenzo-p-dioxins and -furans
PeCDD	pentachlorodibenzo-p-dioxin
PeCDF	pentachlorodibenzofuran
PM	particulate matter
MSWIs	municipal solid waste incinerators
MSW	municipal solid waste
n_i	number of hydrogen atoms substituted by chlorine
η	PCDD/F removal efficiency
NATO/CCMS	North Atlantic Treaty Organization/Committee on the Challenges of Modern Society
r	Pearson correlation coefficient
R	flue gas flow rate (Nm ³ /h)
RDF	refuse-derived fuel
t	reaction time (h or day)
TeCDD	tetrachlorodibenzo-p-dioxin
TeCDF	tetrachlorodibenzofuran

numerous scientific studies have reported the emissions characteristics of PCDD/Fs under transient operations (Gass et al., 2002; Wang et al., 2007a, 2007b). Transient operations can affect the distribution of PCDD/Fs homologues (Grosso et al., 2007) and lead to the memory effect (Syc et al., 2015), wherein PCDD/Fs emissions remain high even after the injection of activated carbon (AC) for 18 h (Wang et al., 2007b). Moreover, the PCDD/Fs emissions under transient operation were mainly formed in the incinerator rather than the post-combustion zone (Tejima et al., 2007). The distribution characteristics of PCDD/Fs and the relationships between PCDD/Fs, chlorobenzenes (CBzs), and polycyclic aromatic hydrocarbons (PAHs) have been investigated under transient conditions (Neuer Etscheidt et al., 2006, 2007; Syc et al., 2015; Tejima et al., 2007; Wang et al., 2007b). However, to the best of our knowledge, studies on the main formation pathways of PCDD/Fs under transient operations have rarely been conducted. Hence, widely applicable reduction strategies for PCDD/Fs in transient operations are lacking.

Optimal reduction strategies under transient operations are an important part of controlling PCDD/Fs emissions throughout the year during MSW incineration. Several effective measures have been carried out for the reduction of PCDD/Fs, including temperature maintenance at 850 °C during start-up and shut-down using auxiliary fuel or natural gas (Chen et al., 2017), and optimization of the electrostatic precipitator operation (Neuer Etscheidt et al., 2006). Cleaning the accumulated ash and shortening the residence time of flue gas can also effectively reduce PCDD/Fs emissions (Cheruiyot et al., 2020). However, PCDD/Fs emissions might exceed the legislative limit, even if these measures are effectively executed (Chen et al., 2017; Cheruiyot et al., 2020). Activated carbon injection (ACI) coupled FF has been considered the most effective method for abating PCDD/Fs emissions (Giugliano et al., 2002). Furthermore, a significant influence of the AC feeding rate on the reduction of dioxin has been reported (Milligan and Altwicker, 1996a, b). Investigating the specific AC feeding rate is critical to accurately control PCDD/Fs emissions to meet the legislation limit for MSWIs under transient operations but current research is still vague in this regard.

In the present study, the formation pathways under transient operations were systematically studied at the individual congener level. First, the relationships between macropollutants (CO, HCl, particulate matter (PM)), tetrachlorodibenzo-p-dioxin (TeCDD) isomers, and

tetrachlorodibenzofuran (TeCDF) isomers were investigated by principal component analysis (PCA). Then, the chlorophenol (CP)-route synthesis, de novo synthesis, CBzs-route synthesis, and the chlorination of dibenzo-p-dioxin (DD)/dibenzofuran (DF) were identified by specific homolog group. Moreover, the main formation pathway was identified by comparing the relative importance and analyzing the relationship between the specific homolog group and PCDD/Fs emissions. Finally, the optimal start-up procedure was constructed by analyzing the main formation pathways and operating conditions, and the optimal feeding rate of AC can be estimated to reduce PCDD/Fs emissions under transient operations.

2. Materials and methods

2.1. Basic information of MSWI and experimental procedures

The study was performed on a continuously operating full-scale MSWI consisting of a circulating fluidized bed (CFB) furnace, a post-combustion chamber with an energy recovery system, and a system of air pollution control devices (APCDs). The system flow diagram of the MSWI and a sampling point is shown in Fig. S1. APCDs include a selective non-catalytic reduction (SNCR), a semi-dry spray neutralizer, an activated carbon injection (ACI) system, and a fabric filter (FF). Besides, the sampling point was at the stack for the PCDD/Fs, CO, PM, and HCl measurements. The crude MSW was converted into refuse-derived fuel (RDF) before entering the incinerator, and the capacity of the CFB is 1200 t/d. No other auxiliary fuel was used during normal operation of the incinerator.

As shown in Fig. S2, the start-up procedure included the cold start-up (cold-start) and hot start-up (hot-start) operation. During the cold-start procedure, diesel was injected to stabilize the incinerator temperature at 300 °C, then biomass and RDF were injected at feeding rate of approximately 15 kg/min to gradually replace diesel while the temperature was maintained at 300 °C in the incinerator. The PCDD/Fs samples were collected after the feeding rate of RDF was 45 kg/min, until the temperature of the incinerator was approximately 800 °C. The detailed sampling process for PCDD/Fs is described in the supplementary material. In addition, before the hot-start procedure, the temperature of the incinerator was 400 °C. The feeding rate of RDF increased from 15 kg/

min to 60 kg/min in 1 h until the temperature was higher than 850 °C. After the start-up procedure, the feeding rate of RDF was kept constant and the incinerator temperature was stabilized for normal operation. The oxygen contents under transient and normal operations are listed in Table 1.

Thirty-one PCDD/Fs samples were collected from the stack gas of the incinerator under normal and transient operations. Eight samples were collected under normal operation within 1 month before the plant shut down. The start-up procedure was constructed by collecting nine samples, including four samples under cold-start (initial temperature of incinerator = 200 °C) and five samples under hot-start (initial temperature of incinerator = 400 °C) operations. Fourteen samples were taken three days after the hot-start operation (the operation defined as “after” start-up), which was accomplished within two days. The sampling time for each flue gas sample during start-up was approximately 1–2 h.

2.2. Sampling and analytical methods

Flue gas samples from the stack were collected iso-kinetically utilizing the KNJ23 stationary source flue gas sampler according to the US EPA method 23a. Details of the pretreatment and analysis method of PCDD/Fs are described in our previous studies (Lin et al., 2020; Yan et al., 2006) and supplementary material. The international toxic equivalent (I-TEQ) of PCDD/Fs was calculated based on North Atlantic Treaty Organization/Committee on the Challenges of Modern Society (NATO/CCMS) factors.

The degree of chlorination of PCDD/Fs is calculated as:

$$d_c = \sum_{i=4}^8 f_i \times n_i \quad (1)$$

where f_i is the weight percentage of PCDD and PCDF congeners and n_i is the number of hydrogen atoms substituted by chlorine.

Temperature, CO, HCl, and PM were simultaneously detected by the flue gas analyzer VarioPlus (MRU GmbH) and soot monitor at the sampling point. In this study, CO, HCl, and PM were classified as macropollutants. The concentrations of the obtained pollutants (PCDD/Fs and macropollutants) were converted to the condition at 11 vol% oxygen content, 1.01×10^5 Pa, and 273 K.

2.3. Statistical analysis

To describe the evolution of the PCDD/Fs-signatures (proportion of specific congeners) under transient operations, the signal intensity of individual congeners was derived according to their weight proportion (wt.%) within their own homolog groups (Chen et al., 2020). For OCDD or OCDF, the contributions were calculated within PCDD or PCDF, respectively. To investigate the relationship between PCDD/Fs, macropollutants, and the average weight proportion of the identified formation pathways, the PCA and Pearson correlation coefficient (r) were adopted. Before PCA, the congener and macropollutant concentrations were normalized to [0,1] using Equation (2).

$$x' = \frac{x - x_{\min}}{x_{\max} - x_{\min}} \quad (2)$$

where x'_i and x_i represent the normalized data and raw data, respectively; x_{\min} and x_{\max} represent the minimum of the raw data and maximum of the raw data, respectively.

2.4. PCDD/Fs reduction model by ACI + FF

AC has been widely applied to adsorb PCDD/Fs emissions from MSWIs. Among APCD units, ACI coupled with FF units can contribute most to the reduction of PCDD/Fs emissions into the atmosphere, including gas-phase PCDD/Fs and solid-phase PCDD/Fs. The PCDD/Fs removal efficiency (η) can be described by a simplified model if dC/dt is a function of C using the first order (Everaert et al., 2003):

$$\frac{dC}{dt} = kAC \quad (3)$$

$$\eta = 1 - \exp(-kAt) \quad (4)$$

where η is defined as $1 - (C_{out}/C_{in})$, and C is the PCDD/Fs concentration; A is a parameter that groups physical characteristics of AC. t is the reaction time and k is the adsorption coefficient. The removal efficiency of PCDD/Fs reduction by ACI + FF includes the gaseous phase (η_1) and solid-phase PCDD/Fs (η_2).

To simplify the reduction model, the parameters in Equation (3) could be assumed to be a function of the AC feeding rate (F (mg/h)) and flue gas flow rate (R (Nm³/h)). The overall removal efficiency is combined with η_1 and η_2 . Therefore, the overall PCDD/F removal efficiency is:

$$\eta = 1 - (1 - \eta_1)(1 - \eta_2) = 1 - \exp(- (k_1^q t_1 + k_2^b t_2)(F/R)) \quad (5)$$

where k_1^q represents $k_1 SA_1$, and k_2^b represents $k_2 fA_2$. In general, t_1 is in the order of magnitude of 1–10 s and t_2 is 0.01–1 s. If the experimental conditions remain constant excluding the AC feeding rate, the parameters are assumed to be reasonably constant.

$$\eta = 1 - \exp(-k_{const}(F/R)) \quad (6)$$

where k_{const} is the apparent constant, which combines the PCDD/Fs removal characteristics in the entrained-phase adsorption and cake-phase filtration with constants t_1 and t_2 .

3. Result and discussion

3.1. PCDD/Fs profiles and macropollutant emissions

3.1.1. PCDD/Fs profiles

Table 1 and Fig. 1(a) show the I-TEQ, PCDD, PCDF, and PCDD/Fs emissions under transient and normal operations. The order of total PCDD/Fs I-TEQ (C_{I-TEQ}) was hot-start (134 ng I-TEQ/Nm³) > cold-start (32 ng I-TEQ/Nm³) > after-start (3.97 ng I-TEQ/Nm³) > normal operation (0.12 ng I-TEQ/Nm³) (Table 1). Furthermore, the PCDD and PCDF

Table 1

PCDD/PCDF ratio, chlorination degree (d_c), I-TEQ, macropollutant concentrations, and oxygen content under transient and normal operation.

Operation condition	Cold start-up		Hot start-up		After start-up		Normal operation	
	Mean	RSD	Mean	RSD	Mean	RSD	Mean	RSD
PCDD/PCDF	2.21	57.4	1.22	9.76	0.91	12.7	0.72	18.4
d_c	4.95	5.76	5.11	0.84	5.31	4.10	5.85	4.52
I-TEQ (ng/Nm ³)	32	63.5	134	41.4	3.97	69.3	0.12	24.9
CO (mg/m ³)	45.0	109	32.1	91.2	10.1	96.0	3.22	44.5
Dust (mg/m ³)	9.6	11.2	11.6	7.48	8.46	15.4	7.77	21.9
HCl(mg/m ³)	18.5	138	9.05	44.3	15.0	12.2	12.1	99.5
O ₂ (vol%)	10.5	6.83	8.48	4.23	5.71	1.73	5.89	1.67

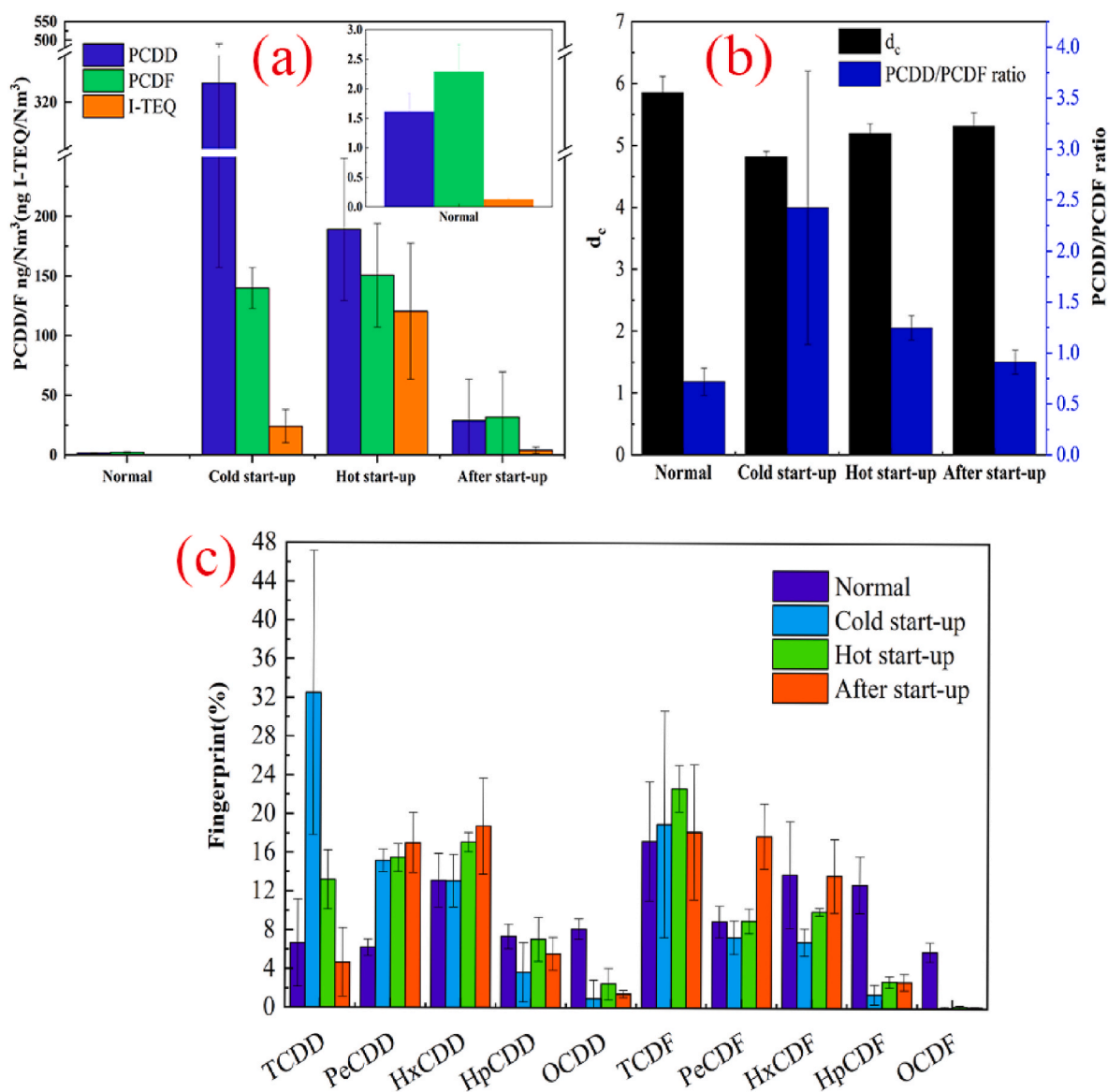


Fig. 1. (a) PCDD/Fs concentrations; (b) degrees of chlorination and ratios of PCDD/PCDF; (c) homolog profiles of PCDD/Fs in normal and transient operations.

emissions of transient operation were far higher than those of normal operation (Fig. 1). The results suggest that the transient operation can significantly promote PCDD/Fs formation. These outcomes are consistent with previous findings on start-up operations (Lin et al., 2014). Specifically, the PCDD, PCDF, and I-TEQ concentrations under cold-start were 200, 70, and 266-fold higher than those under normal operation. These results can be attributed to poor combustion and the temperature window (200–600 °C) for dioxin formation during the start-up procedure, which remarkably contributes to PCDD/F formation (Addink et al., 1998; Aurell et al., 2009). The increase in PCDD/Fs emissions under transient operations was found to be higher than that reported in previous studies (Li et al., 2017; Syc et al., 2015). There are two possible reasons for this observation. First, the low mass transfer rate between oxygen and RDF limits the complete combustion of the carbon matrix and soot, owing to the large amount of RDF injected within 1 h. Second, poor combustion is more likely to occur during the start-up procedure of large-scale incinerators. Moreover, the C_{I-TEQ} of hot-start was four-fold higher than that of cold-start (Table 1) (Gullett et al., 2012). However, as shown in Fig. 1(a), the total PCDD/Fs concentrations (136 congener concentrations) at hot-start are far lower than those at cold-start. These results indicate that hot-start operation can promote the formation of 2,

3,7,8-substituted PCDD/Fs.

Homolog profiles of PCDD/Fs during the transient and normal operations are shown in Fig. 1(c). The proportion of OCDD under transient operations (0.05%, 0.21%, and 0.15% for cold-start, hot-start, and after-start operations, respectively) was lower than that under normal operation (5.85%). Under cold-start operation, the proportion of TeCDD (32.5%) was remarkably higher than that under the other operations (6.7%, 13.2%, and 4.7% for normal, hot-start, and after-start operation, respectively). Fig. 2 shows the fingerprints of PCDD/Fs congeners during transient and normal operations. The fingerprints of transient operation differ from those of normal operation. Furthermore, the chlorination degrees were 4.81, 5.19, and 5.31 under cold-start, hot-start, and after-start operations, respectively (Table 1). The chlorination degrees under transient operation are lower than those under normal operation (5.85). These results indicate that transient operation might facilitate the formation of low-chlorinated congeners rather than high-chlorinated congeners. Moreover, the high PCDD/Fs emissions under the after-start operation indicate that the memory effect caused by start-up can occur in the incinerator without wet scrubbers or aged fabric filters.

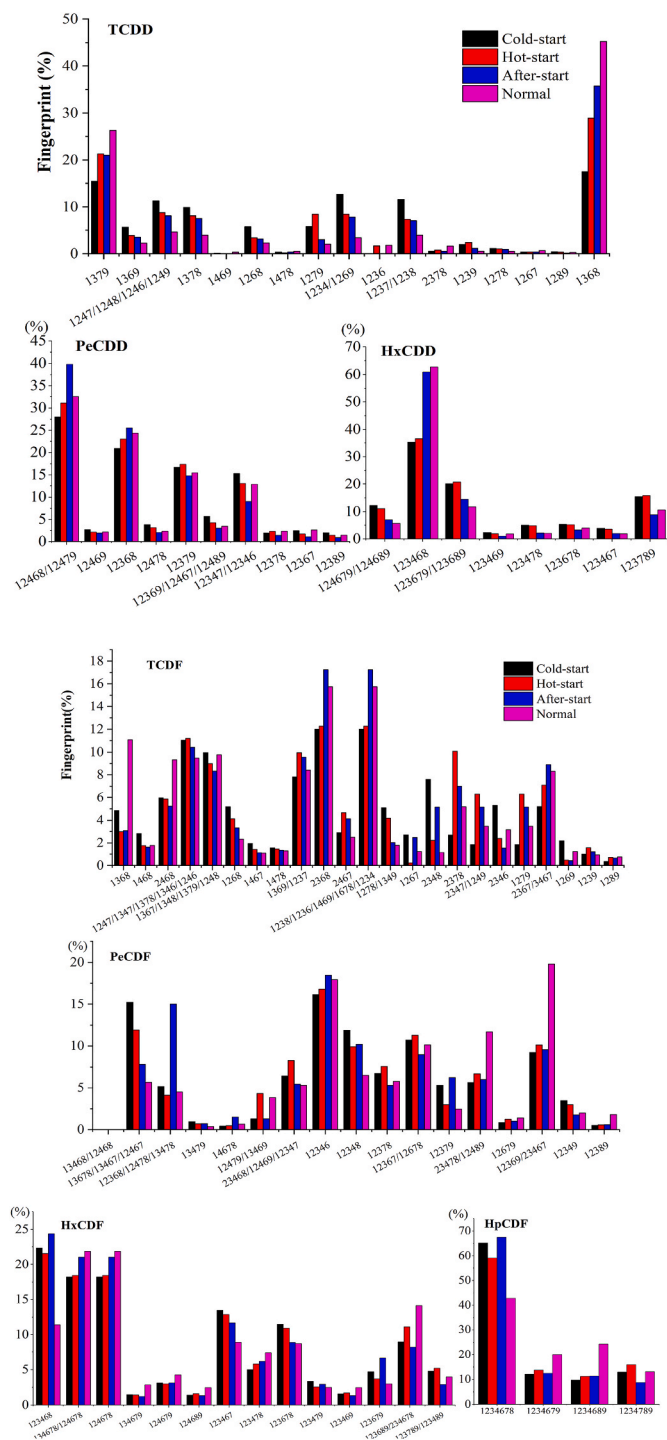


Fig. 2. Fingerprints of PCDD/F congeners in transient and normal operations.

3.1.2. Macropollutant emissions

Macropollutants are directly correlated with a carbon (Kaune et al., 1994; Oh et al., 1999) and chlorine sources for PCDD/Fs formation (Olie et al., 1998). Table 1 lists the macropollutant emissions under transient and normal operations. Fig. 3(e), (f), (g), and(h) present the concentrations of CO, PM, and HCl under transient operation. Under cold-start operation, the CO, PM, and HCl concentrations decreased as the incinerator temperature increased. As shown in Fig. S3, the CO emissions decreased in the following order: cold-start (45.0 mg/Nm³), hot-start (32.1 mg/Nm³), after-start (10.1 mg/Nm³), and normal operation (3.22 mg/Nm³). The trend of CO emissions was consistent with that of

PCDD concentrations (Fig. 1(a)). Hence, the abundant carbon matrix deduced by high CO concentrations (Kaune et al., 1994; Oh et al., 1999) can be an important carbon source for PCDD formation under transient operation. Even if the temperature of incinerator exceeds 850 °C under after-start operation, the CO concentrations can be higher than those under the normal operation. This finding indicates that the deposited soot can be oxidized to CO and other organic pollutants, such as polychlorinated biphenyl, chlorophenol, and PCDD/Fs, under after-start operation (Syc et al., 2015).

3.2. Evolution of PCDD/F-signatures

For the main PCDD/Fs emissions from MSWI, three main pathways were identified: de novo synthesis (Addink et al., 1998; Hell et al., 2001a), precursor formation (Ryu et al., 2005b; Shadrack, 2014), and chlorination of DD/DF (Tuppurainen et al., 2003). PCDD/Fs are formed from organic carbon or PAHs in de novo synthesis through heterogeneous reaction (200–400 °C) (Hell et al., 2001a). Besides, the main precursor formation includes CBzs-route synthesis and CP-route synthesis. Due to the significant importance of 2,3,7,8-substitutions, the chlorination of DD/DF was considered.

3.2.1. Relationship among TeCDD/TeCDF isomers and macropollutants

The results of the laboratory experiments on the isomer distribution of TeCDD formed from chlorinated phenols by gas-phase reactions/pyrolysis were widely consistent. Thus, several researchers have inferred the formation pathways of PCDD/Fs by giving detailed information on the TeCDD (Neuer Etscheidt et al., 2007; Swerev and Ballschmiter, 1989; Wehrmeier et al., 1998). TeCDF isomers are considered important congeners because they contribute approximately 20% to PCDD/Fs emissions under transient and normal operations (Fig. 1(c)). As shown in Fig. 3, PCA was used to investigate the relationship between TeCDD/TeCDF isomers and macropollutants under hot-start, after-start, and normal operations. As shown in Figs. 1(a) and Fig. 2, the PCDD/Fs emissions and fingerprints of cold-start are nearly consistent with those of hot-start operation. Therefore, it is reasonable to only analyze the relationship for hot-start operation. Under the normal operations (Fig. 4(a) and (b)), the cumulative variance contribution rates of the first two factors were only 67.2% and 66.8% for TeCDF and TeCDD, respectively. The TeCDD/TeCDF isomers were dispersedly distributed in the first and second quadrants. Moreover, the cumulative variance contribution rates of the first two factors under transient operations (hot-start: 89.1% and 88.1%; after-start: 92.6% and 89.9% for TeCDF or TeCDD, respectively) were higher than those under normal operations. These results suggest a strong correlation between TeCDD or TeCDF isomers under transient operations.

For normal operation, there is strong positive correlation among 1278-(1379-), 2367-(3467-), 2346-(1249-) TeCDF and PM (Fig. 4(a)). In addition, 1236-TeCDD was positively correlated with CO and PM concentrations (Fig. 3(b)). For the hot-start operation, a positive relationship was found among 1268- and 1234-TeCDD, PM and CO (Fig. 4(c)). Other TeCDD isomers were aggregated in the first quadrant, while 1267- and 2378-TeCDD were far from the other TeCDD isomers and distributed in the second quadrant. Furthermore, 1239-/1236/2378-TeCDF, showed a weak correlation with the other TeCDF isomers (Fig. 4(d)). Under the after-start operation, all TeCDD/TeCDF isomers aggregated, indicating a strong correlation among the vast number of TeCDF/TeCDD isomers. Fig. 4(e) and (f) show that CO and PM are negatively correlated with the TeCDD/TeCDF isomers.

As shown in Table 2, the PM has a significantly negative correlation coefficient ($r = -0.852$) with PCDD/Fs emissions under the after-start operation. For after-start operation, the PCDD/Fs emissions are mainly due to the memory effect of the aged FF, wet scrubbers, or other APCDs (Trivedi and Majumdar, 2013). The results demonstrate that an increase in PM can prevent PCDD/Fs from being desorbed from the APCDs. Moreover, the HCl concentration was positively correlated with

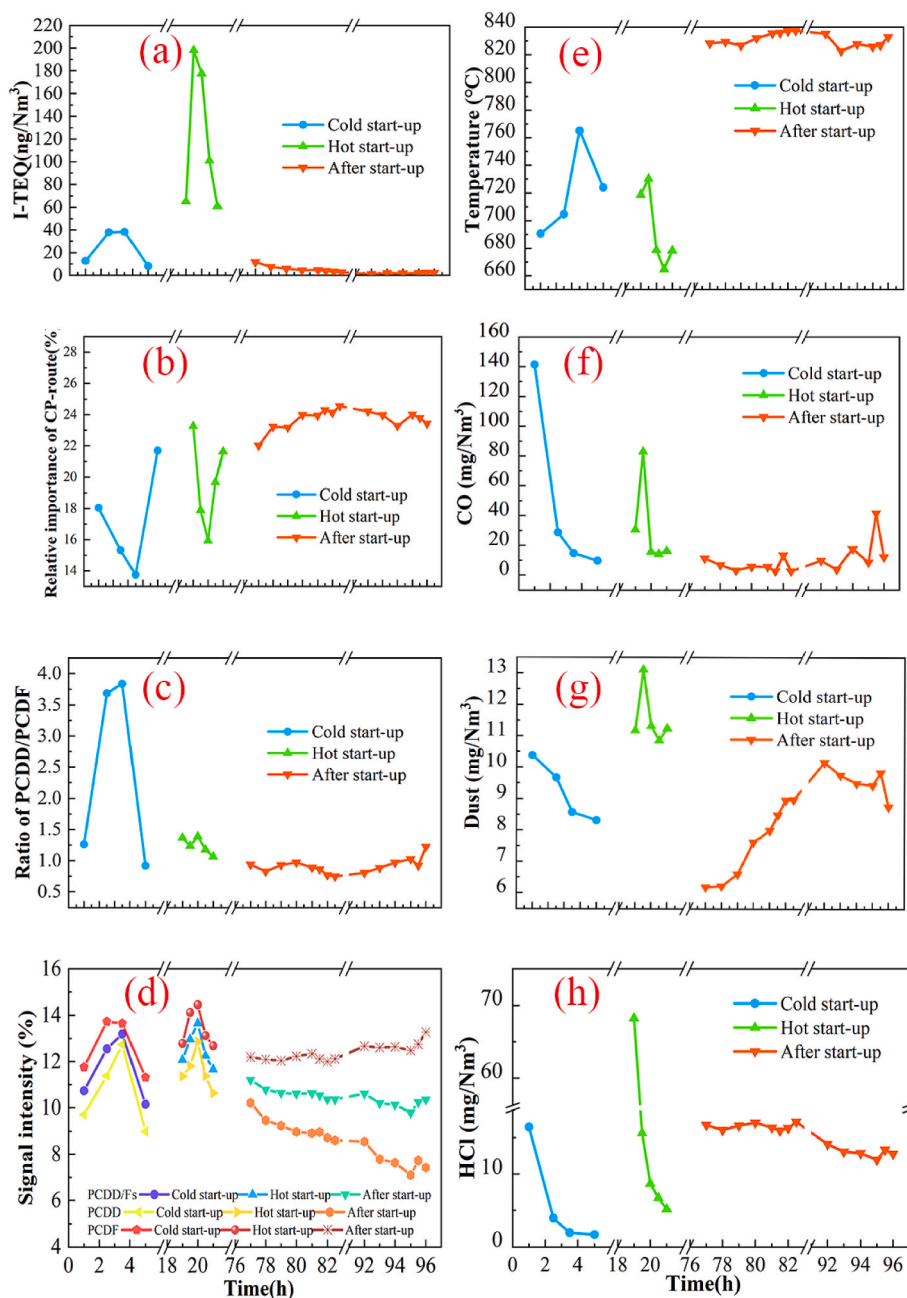


Fig. 3. Trend of (a) I-TEQ, (b) the relative importance of the CP-route, (c) PCDD/PCDF ratio, (d) the trend of DD signal-intensity ($PCDD_{avr}$), DF signal-intensity ($PCDF_{avr}$) and average DD/DF signal-intensity ($PCDD/F_{avr}$), (e) incinerator temperature, (f) CO, (g) PM, (h) HCl concentration under transient operations (cold-start, hot-start, and after-start).

PCDD/Fs emissions under after-start ($r = 0.449$). These findings indicated that HCl promoted the formation of PCDD/Fs.

3.2.2. De novo synthesis and CBzs-route synthesis

For de novo synthesis, PCDF is easier to form than PCDD (McKay, 2002), and catalytic metals accelerate the reaction rate of de novo synthesis (Olie et al., 1998). In addition, the ratio of PCDD to PCDF is similar in CBzs-route synthesis (Shadrack, 2014). Hence, the PCDD/Fs emissions from de novo synthesis and CBzs-route synthesis can be inferred from the ratio of PCDD/PCDF.

As shown in Figs. 1(b) and Fig. 3(c), the ratio of PCDD/PCDF was 2.43, 1.25, 0.91, and 0.72 under cold-start, hot-start, after-start, and normal operations, respectively. These results indicate that the PCDD/Fs emissions are mainly derived de novo synthesis and CBzs-route synthesis

under after-start and the normal operation. However, the ratios of PCDD/PCDF are larger than 1 under cold-start and hot-start operations, aligning well with existing studies on PCDD/Fs emissions under cold-start operation (Wang et al., 2007b). Fig. S2 shows the initial incinerator temperature during the start-up period was above 400 °C, and the average incinerator temperature was approximately 600 °C. The temperature was higher than the temperature window (200–400 °C) for de novo synthesis. Hence, the contribution of de novo synthesis and CBzs-route synthesis to PCDD/Fs is low under cold-start and hot-start operations. Moreover, our findings are somewhat surprising since the ratio of PCDD/PCDF has a highly positive coefficient with PCDD/Fs emissions ($r = 0.93$) under the cold-start operation. This is possibly because the dominant PCDD/Fs emissions are PCDD during the cold-start period. Moreover, the ratio of PCDD/PCDF had weak

Table 2

Pearson coefficients between PCDD/Fs concentrations with macropollutants (CO, PM, HCl), the relative importance of the CP-route, the ratio of PCDD/PCDF, degree of chlorination, the average signal intensity of DD, the average signal intensity of DF, and the average signal intensity of DD/DF under transient and normal operation.

Coefficients	Normal operation	cold-start	hot-start	after-start
CO	0.417	-0.405	0.594	-0.174
PM	-0.369	0.059	0.655	-0.852 ^c
HCl	-0.559	-0.401	-0.298	0.449
CP-route	0.573	-0.791	-0.845 ^b	-0.827 ^c
d _c	-0.739 ^b	0.302	-0.611	-0.661 ^b
PCDD/PCDF ratio	-0.21	0.93 ^a	0.399	-0.007
PCDD _{avr}	-0.067	0.774	0.756	0.747 ^c
PCDF _{avr}	0.125	0.948 ^b	0.909 ^a	-0.42
PCDD/F _{avr}	0.066	0.862	0.853 ^b	0.752 ^c

Note: a means p-value ≤ 0.05; b means 0.05 < p value ≤ 0.01; c means p value < 0.005; no marks mean p-value > 0.1.

correlation with PCDD/Fs emissions for normal operation ($r = -0.21$), hot-start ($r = 0.399$), and after-start ($r = -0.007$).

3.2.3. CP-route synthesis

CPs are considered a rather important precursor as PCDD/Fs can be directly formed in CP-route synthesis (Nganai et al., 2009, 2012). In addition, CPs were reported to be abundant in MSW incinerators (Weber and Hagenmaier, 1999). As shown in Table 3, eight specific PCDD/Fs congeners can be identified as typical congeners for CP-route synthesis (Chen et al., 2020) owing to their evident proportion. Specific PCDD/Fs congeners include 1379-,1368-TeCDD isomers (Mulholland et al., 2001; Sidhu et al., 1995), 12468-, 12368-,12379-PeCDD, 123,468-(123,479-) HxCDD (Tuppurainen et al., 2003; Zhang et al., 2017), and 2468-, 1238+-TeCDF (Blaha and Hagenmaier, 1995; Ryu et al., 2005a). Further, the relative importance values were used to describe the contribution of each congener (%) within its homolog group for each sample. The relative importance and details of the CP-route congeners are shown in Tables S1-S4.

The relative importance of the CP-route synthesis under transient and normal operations is summarized in Table 3 and Fig. S4, including the mean and standard deviation. The relative importance of CP-route synthesis increased in the order: cold-start (18.4%), hot-start (18.8%), after-start (23.7%), and normal operation (24.0%). The proportion of PCDD/Fs synthesized by the CP-route decreased under transient operation, and the relative importance of the CP-route synthesis under after-start condition was close to that under normal operations. Moreover, as shown in Fig. 3(a) and (b), the trend of the relative importance of the CP-route during the cold-start period is the same as that during the hot-start period, first rising and then declining to the level of the after-start operation. Therefore, the contribution of CP-route synthesis to PCDD/Fs can be considered consistent for cold-start and hot-start operations.

Table 3

Relative importance of CP-route congeners under transient and normal operation.

Congeners	Cold start-up		Hot start-up		After start-up		Normal operation	
	mean	std	mean	std	mean	std	mean	std
1379-TeCDD	18.04	3.37	21.52	1.42	18.16	1.97	22.08	5.01
1368-TeCDD	23.38	8.38	30.06	5.64	38.73	2.48	41.61	4.36
Sum, % of TeCDD	41.42	11.54	51.58	6.85	56.89	2.78	63.69	9.15
12,468+-PeCDD	15.53	2.95	15.60	1.99	19.22	1.87	16.27	0.55
12368-PeCDD	22.61	3.17	23.10	2.07	25.24	0.70	24.54	1.20
12379-PeCDD	16.62	1.01	17.47	0.83	14.76	0.41	15.51	1.04
Sum, % of PeCDD	54.76	6.14	56.16	3.94	59.21	2.50	56.31	1.63
123468-HxCDD	42.91	12.27	34.70	6.02	65.13	4.78	62.59	2.18
2468-TeCDF	5.84	0.21	5.88	0.12	4.66	0.50	6.62	4.86
1238+-TeCDF	2.35	0.52	2.00	0.36	3.86	0.68	3.01	0.75
Sum, % of TeCDF	8.19	0.36	7.88	0.30	8.52	0.44	9.64	4.24
Average	18.41	3.63	18.79	2.11	23.72	0.62	24.03	1.73

Specifically, 123468-HxCDD contributes most to the difference in the relative importance of CP-route synthesis between cold-start/hot-start and normal operation. The relative importance of the CP-route trend is opposed that of the PCDD/Fs concentrations under transient operations. Furthermore, the CP-route synthesis was negatively correlated with PCDD/Fs emissions under transient conditions ($r = -0.791$ for cold-start, $r = -0.845$ for hot-start, and $r = -0.827$ for after-start). The results indicate that CP-route synthesis contributes slight to the increase of PCDD/Fs emissions. For normal operations, a positive correlation ($r = 0.573$) was found between the relative importance of CP-route synthesis and PCDD/Fs emissions. This outcome indicates that the contribution to PCDD/Fs emissions from CP-route synthesis is positive under normal operations.

3.2.4. Chlorination of DD/DF

The chlorination of DD/DF is a potential source of the PCDD/Fs emissions (Hagenmaier et al., 1987). For the congeners synthesized from DD/DF, 2,3,7,8-position PCDD congeners are representatives of DD chlorination (Wehrmeier et al., 1998), while 2,3,7,8-position PCDF congeners are representatives of DF chlorination (Ryu et al., 2003), based on the signal intensity. The signal intensity of chlorination of DD/DF (Hagenmaier profile) is displayed in Tables S5-S8 for transient and normal operations.

A summary of the Hagenmaier profiles under transient and normal operations is presented in Table S9 and Fig. S4. The average signal intensity under normal operation (13.48%) was higher than that under transient operation (11.66% under cold-start, 12.52% under hot-start, and 10.46% under after-start). This outcome indicates that the contribution to PCDD/Fs emissions from the chlorination of DD/DF under normal operations is higher than that under transient operations. As shown in Fig. 3(d), the signal intensity of chlorination of DD/DF under cold-start is consistent with that under hot-start, declining first and then rising to the of after-start level. Under after-start, the average signal intensity of DD chlorination remained nearly constant, whereas the average signal intensity of DF chlorination declined. These results indicate that DD is more easily chlorinated than DF under after-start condition. Furthermore, the average signal intensity of DD/DF chlorination and the ratio of PCDD/PCDF were consistent with the changing trend in the incinerator temperature. Hence, incinerator temperature is a crucial factor for the de novo synthesis and chlorination of DD/DF. Under after-start operation, the trend of the average signal intensity of DF chlorination was consistent with the trend of C_{L-TEQ} (Fig. 3(a), (d)). This finding indicates that the contribution of the DF chlorination to I-TEQ is higher than that of DD chlorination. Table 2 shows the Pearson coefficient between the PCDD/Fs concentrations and chlorination of DD/DF. The average signal intensity of the DD/DF chlorination was strongly positively correlated with the PCDD/Fs emissions under transient operations ($r = 0.862$ for cold-start, $r = 0.853$ for hot-start, and $r = 0.752$ for after-start). In contrast, for normal operation, the average

signal intensity of DD/DF chlorination is weakly correlated with the PCDD/Fs emissions. Towing to the high correlation coefficients ($R^2 = 0.76$) between HCl concentrations and average signal intensity of DD chlorination in Fig. S5, HCl can be considered a key influence factor for DD chlorination under after-start operation.

3.3. Optimal start-up procedure

Fig. 5 shows main formation pathways and optimal reduction strategies for extreme PCDD/Fs emissions under transient operations. In particular, the main products of the CP-route synthesis are PCDD. However, the cold-start PCDD emissions are as high as 543 ng/Nm^3 . PCDD can also be formed by the direct release of carbon matrix oxidation without metal catalysts (Grandesso et al., 2008; Hell et al., 2001b). Therefore, the formation of PCDD is mainly from the carbon matrix oxidation under cold-start and hot-start operations. In contrast to the typical formation of PCDD/Fs dominated by de novo and precursor synthesis, the signatures of PCDD/Fs from de novo synthesis, precursor formation, and chlorination of DD/DF under transient operations are reduced. The results indicate that the PCDD/Fs emissions are mainly from carbon matrix oxidation under transient operations owing to the vast incomplete combustion products. Therefore, the minimization of soot deposition and reaction time are crucial measures for suppressing PCDD/Fs formation under transient operations. The time for the hot-start procedure was 2 h, which was shorter than that for the cold-start procedure (4 h). Hence, for the hot-start operation, the feeding rate of the RDF and temperature of the incinerator increased more rapidly. A shorter start-up time can promote the formation of 2,3,7,8-substituted PCDD/Fs (17 toxic congeners) but will suppress other PCDD/Fs congeners (Wang et al., 2007a). Combined with the PCDD/Fs kinetic formation studies (Grandesso et al., 2008; Lasagni et al., 2009), minimization of soot deposition and reaction time are crucial measures to suppress PCDD/Fs formation. Therefore, during the start-up period, the RDF should be evenly injected rather than applying a large amount in a short time to prevent the formation of a large amount of soot or carbon matrix. Further, the oxygen content for the incineration should be increased (>8%) to suppress PCDD/Fs formation from large amounts of macromolecular carbon and incomplete combustion products during the start-up procedure.

3.4. Optimal injection rate of AC

As shown in Fig. S6, for the after-start operation, the C_{I-TEQ} decreased rapidly and then gradually decreased over time in the CFB and grate furnace. The trend of C_{I-TEQ} on the reaction time is similar to the

dependence of carbon concentration on the reaction time (Grandesso et al., 2008). Moreover, the R^2 of the power function fitting for the I-TEQ and time after start-up was as high as 0.97 in the work. For the dataset (Syc et al., 2015) with a grate furnace, the power was -0.59 , near that of the CFB (-0.65). These results suggest that the PCDD/Fs emissions under after-start operation may follow a certain power function regardless of the type of incinerator. As a result, the PCDD/Fs emissions can be described as:

$$I - TEQ = const * t^{-0.65} \quad (7)$$

where t is the time after start-up (h/d); however, the variable $const$ is different between CFB and the grate furnace. This difference may be due to the time interval and the incinerator type. Hence, the feeding rate of AC can be calculated by substituting Equation (7) into Equation (5), and is expressed as follow:

$$F = \frac{R}{k_{const}} \ln \left(\frac{C_{out}}{const * t^{-0.65}} \right) \quad (8)$$

Under after-start operation, the feeding rate of the AC can be determined by Equation (8). If the flue gas flow rate is known and the dioxin concentration in the flue gas of FF outlet is assumed as the emission limits ($0.1 \text{ ng I-TEQ/Nm}^3$), the optimal feeding rate of AC can be estimated using k_{const} and $const$. For instance (Chang et al., 2009), expressed Equation (8) using a semi-empirical Equation (9):

$$\eta(\%) = \frac{100}{\left[1 + \left(40.2(F/R)^3 \right) \right]} \quad (R^2 = 0.9269) \quad (9)$$

Thereafter, the feeding rate of AC for CFB to control the $C_{out} = 0.1 \text{ ng I-TEQ/Nm}^3$ can be expressed as:

$$F / R = 277 (11.72t^{-0.65} - 0.1)^{\frac{1}{3}} \quad (10)$$

For the grate furnace, the feeding rate of AC can be expressed as:

$$F / R = 277 (4.21t^{-0.59} - 0.1)^{\frac{1}{3}} \quad (11)$$

Therefore, Equations (10) and (11) can be applied to the PCDD/Fs emission reduction under after-start operations, considering that the flue gas flow rate is known. Therefore, PCDD/Fs emissions can be reduced to the national legislation limit with the optimal injection rate of AC by the time after start-up. As for the region with the strictest criterion with $0.05 \text{ ng I-TEQ/Nm}^3$, then equations (10) and (11) can be modified by assuming $C_{out} = 0.05 \text{ ng I-TEQ/Nm}^3$.

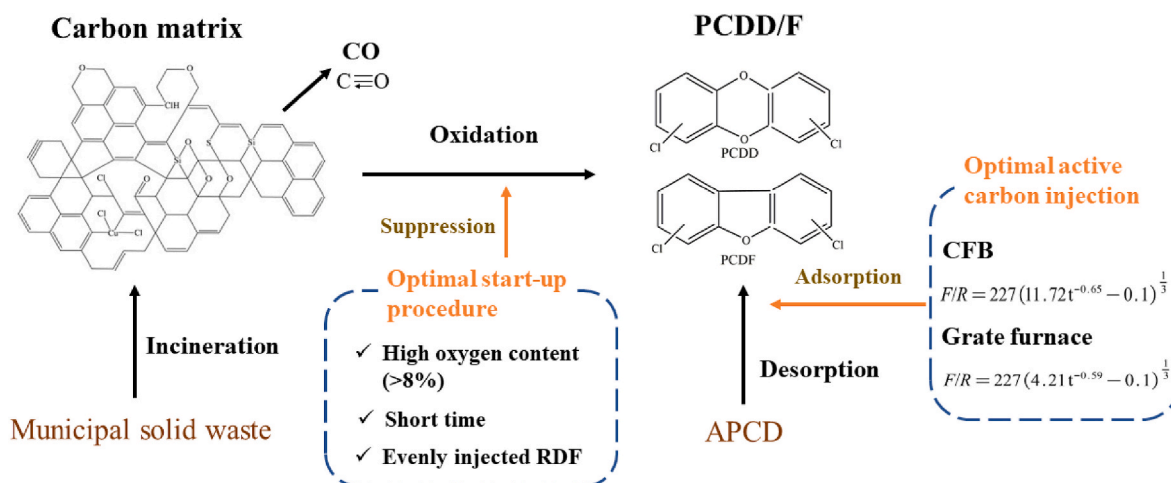


Fig. 5. Formation pathways of PCDD/F and optimal reduction strategies for extreme PCDD/Fs emissions under transient operations.

4. Conclusions

Statistical analysis of the evolution of PCDD/Fs congeners and macropollutants revealed and verified the formation pathways of PCDD/Fs. Finally, the optimal start-up procedure and optimal feeding rate of AC were established to control the PCDD/Fs emissions to the legislation limit. The results are as follows:

- (1) The extreme PCDD/Fs emissions under transient operation are 120-fold higher than those under normal operations. The transient operations facilitate the formation of lowly chlorinated congeners at a higher level than highly chlorinated congeners.
- (2) The abundant carbon matrix can be an important carbon source for PCDD formation. Oxidation of the carbon matrix is the main source of PCDD/Fs emissions, compared with de novo synthesis, CBzs-route synthesis, CP-route synthesis, and chlorination of DD/DF.
- (3) Evenly feeding waste, high oxygen content (>8%), and short time for start-up procedure can effectively reduce PCDD/Fs emissions.
- (4) The optimal feeding rate of AC can be estimated by the I-TEQ-time equations and semi-empirical equations of PCDD/Fs reduction to control PCDD/F emissions to 0.1 ng I-TEQ/Nm³.

The formation pathways of PCDD/Fs under transient operation were revealed, and the optimal reduction strategies can be constructed to control the PCDD/Fs emissions to 0.1 ng I-TEQ/Nm³ from MSWI under transient operations.

Author statement

Shijian Xiong: Conceptualization, Methodology, Software, Data curation, Writing- Original draft. **Yaqi Peng:** Writing-Reviewing. **Shengyong Lu:** Writing-Reviewing and Supervision. **Ken Chen:** Validation, Software. **Xiaodong Li:** Supervision. **Kefa Cen:** Supervision.

Declaration of competing interest

The authors declare that they have no known competing financial interests or personal relationships that could have appeared to influence the work reported in this paper.

Acknowledgments

This research is supported by the National Key Research and Development Program of China (2020YFE0107600).

Appendix A. Supplementary data

Supplementary data to this article can be found online at <https://doi.org/10.1016/j.jenvman.2022.114878>.

References

Addink, R., Govers, H.A.J., Olie, K., 1998. Isomer distributions of polychlorinated dibenzo-p-dioxins/dibenzofurans formed during de novo synthesis on incinerator fly ash. *Environ. Sci. Technol.* 32, 1888–1893.

Aurell, J., Fick, J., Marklund, S., 2009. Effects of transient combustion conditions on the formation of polychlorinated dibenzo-p-dioxins, dibenzofurans, and benzenes, and polycyclic aromatic hydrocarbons during municipal solid waste incineration. *Environ. Eng. Sci.* 26, 509–520.

Blaha, J., Hagenmaier, H., 1995. Time dependence of the de novo synthesis of PCDD/PCDF and potential precursors on a model fly ash. *Organohalogen Compd* 23, e406.

Chang, Y.M., Hung, C.Y., Chen, J.H., Chang, C.T., Chen, C.H., 2009. Minimum feeding rate of activated carbon to control dioxin emissions from a large-scale municipal solid waste incinerator. *J. Hazard Mater.* 161, 1436–1443.

Chen, C.Y., Lee, W.J., Mwangi, J.K., Wang, L.C., Wu, J.L., Lin, S.L., 2017. Reduction of persistent organic pollutant emissions during incinerator start-up by using crude waste cooking oil as an alternative fuel. *Aerosol Air Qual. Res.* 17, 899–912.

Chen, Z., Zhang, S., Lin, X., Li, X., 2020. Decomposition and reformation pathways of PCDD/Fs during thermal treatment of municipal solid waste incineration fly ash. *J. Hazard Mater.* 394, 122526.

Cheruiyot, N.K., Yang, H.H., Wang, L.C., Lin, C.C., 2020. Feasible and effective control strategies on extreme emissions of chlorinated persistent organic pollutants during the start-up processes of municipal solid waste incinerators. *Environ. Pollut.* 267, 115469.

Everaert, K., Baeyens, J., Creemers, C., 2003. Adsorption of dioxins and furans from flue gases in an entrained flow or fixed/moving bed reactor. *J. Chem. Technol. Biotechnol.* 78, 213–219.

Gass, H.C., Lüder, K., Wilken, M.J.O.c., 2002. PCDD/F- emissions during cold start-up and shut-down of a municipal waste incinerator 56, 193–196.

Giugliano, M., Cernuschi, S., Grosso, M., Miglio, R., Aloigi, E., 2002. PCDD/F mass balance in the flue gas cleaning units of a MSW incineration plant. *Chemosphere* 46, 1321–1328.

Grandesso, E., Ryan, S., Gullett, B., Touati, A., Collina, E., Lasagni, M., Pitea, D., 2008. Kinetic modeling of polychlorinated dibenzo-p-dioxin and dibenzofuran formation based on carbon degradation reactions. *Environ. Sci. Technol.* 42, 7218–7224.

Grosso, M., Cernuschi, S., Giugliano, M., Lonati, G., Rigamonti, L., 2007. Environmental release and mass flux partitioning of PCDD/Fs during normal and transient operation of full scale waste to energy plants. *Chemosphere* 67, S118–S124.

Gullett, B.K., Oudejans, L., Tabor, D., Touati, A., Ryan, S., 2012. Near-real-time combustion monitoring for PCDD/PCDF indicators by GC-REMPI-TOFMS. *Environ. Sci. Technol.* 46, 923–928.

Hagenmaier, H., Kraft, M., Brunner, H., Haag, R., 1987. Catalytic effects of fly ash from waste incineration facilities on the formation and decomposition of polychlorinated dibenzo-p-dioxins and polychlorinated dibenzofurans. *Environ. Sci. Technol.* 21, 1080–1084.

Hell, K., Stieglitz, L., Dinjus, E., 2001a. Mechanistic aspects of the de-novo synthesis of PCDD/PCDF on model mixtures and MSWI fly ashes using amorphous 12C- and 13C-labeled carbon. *Environ. Sci. Technol.* 35, 3892–3898.

Hell, K., Stieglitz, L., Dinjus, E., 2001b. Mechanistic aspects of the de-novo synthesis of PCDD/PCDF on model mixtures and MSWI fly ashes using amorphous C-12- and C-13-labeled carbon. *Environ. Sci. Technol.* 35, 3892–3898.

Huang, Y., Chen, Y., Li, Y., Zhou, L., Zhang, S., Wang, J., Du, W., Yang, J., Chen, L., Meng, W., Tao, S., Liu, M., 2021. Atmospheric emissions of PCDDs and PCDFs in China from 1960 to 2014. *J. Hazard Mater.* 424, 127320.

Kaune, A., Lenoir, D., Nikolai, U., Kettrup, A., 1994. Estimating concentrations of polychlorinated dibenzo-p-dioxins and dibenzofurans in the stack gas of a hazardous-waste incinerator from concentrations of chlorinated benzenes and biphenyls. *Chemosphere* 29, 2083–2096.

Lasagni, M., Collina, E., Grandesso, E., Piccinelli, E., Pitea, D., 2009. Kinetics of carbon degradation and PCDD/PCDF formation on MSWI fly ash. *Chemosphere* 74, 377–383.

Li, M., Wang, C., Cen, K., Ni, M., Li, X., 2017. PCDD/F emissions during startup and shutdown of a hazardous waste incinerator. *Chemosphere* 181, 645–654.

Lin, X., Huang, Q., Chen, T., Li, X., Lu, S., Wu, H., Yan, J., Zhou, M., Wang, H., 2014. PCDD/F and PCBz emissions during start-up and normal operation of a hazardous waste incinerator in China. *Aerosol Air Qual. Res.* 14, 1142–1151.

Lin, X., Ma, Y., Chen, Z., Li, X., Lu, S., Yan, J., 2020. Effect of different air pollution control devices on the gas/solid-phase distribution of PCDD/F in a full-scale municipal solid waste incinerator. *Environ. Pollut.* 265, 114888.

Lu, S., Xiang, Y., Chen, Z., Chen, T., Lin, X., Zhang, W., Li, X., Yan, J., 2021. Development of phosphorus-based inhibitors for PCDD/Fs suppression. *Waste Manag.* 119, 82–90.

McKay, G., 2002. Dioxin characterisation, formation and minimisation during municipal solid waste (MSW) incineration: review. *Chem. Eng. J.* 86, 343–368.

Milligan, M.S., Altwicker, E.R., 1996a. Chlorophenol reactions on fly ash. 1. Adsorption/desorption equilibria and conversion to polychlorinated dibenzo-p-dioxins. *Environ. Sci. Technol.* 30, 225–229.

Milligan, M.S., Altwicker, E.R., 1996b. Chlorophenol reactions on fly ash. 2. Equilibrium surface coverage and global kinetics. *Environ. Sci. Technol.* 30, 230–236.

Mulholland, J.A., Akki, U., Yang, Y., Ryu, J.-Y., 2001. Temperature dependence of DCDD/F isomer distributions from chlorophenol precursors. *Chemosphere* 42, 719–727.

Neuer Etscheidt, K., Nordsieck, H.O., Liu, Y.B., Kettrup, A., Zimmermann, R., 2006. PCDD/F and other micropollutants in MSWI crude gas and ashes during plant start-up and shut-down processes. *Environ. Sci. Technol.* 40, 342–349.

Neuer Etscheidt, K., Orasche, J., Nordsieck, H., Streibel, T., Zimmermann, R., Kettrup, A., 2007. Changes in PCDD/PCDF formation processes during instationary phases of combustor operation - exemplified by the use of C14DD isomer patterns. *Chemosphere* 67, S205–S216.

Nganai, S., Lomnicki, S., Dellinger, B., 2009. Ferric oxide mediated formation of PCDD/fs from 2-monochlorophenol. *Environ. Sci. Technol.* 43, 368–373.

Nganai, S., Lomnicki, S., Dellinger, B., 2012. Formation of PCDD/Fs from oxidation of 2-monochlorophenol over an Fe2O3/silica surface. *Chemosphere* 88, 371–376.

Oh, J.E., Lee, K.T., Lee, J.W., Chang, Y.S., 1999. The evaluation of PCDD/Fs from various Korean incinerators. *Chemosphere* 38, 2097–2108.

Olie, K., Addink, R., Schoonenboom, M., 1998. Metals as catalysts during the formation and decomposition of chlorinated dioxins and furans in incineration processes. *J. Air Waste Manag. Assoc.* 48, 101–105.

Qiu, J., Tang, M., Peng, Y., Lu, S., Li, X., Yan, J., 2020. Characteristics of PCDD/fs in flue gas from MSWIs and HWIs: emission levels, profiles and environmental influence. *Aerosol Air Qual. Res.* 20, 2085–2097.

Ryu, J.-Y., Mulholland, J.A., Takeuchi, M., Kim, D.-H., Hatanaka, T., 2005a. CuCl₂-catalyzed PCDD/F formation and congener patterns from phenols. *Chemosphere* 61, 1312–1326.

- Ryu, J.Y., Mulholland, J.A., Chu, B., 2003. Chlorination of dibenzofuran and dibenzo-p-dioxin vapor by copper (II) chloride. *Chemosphere* 51, 1031–1039.
- Ryu, J.Y., Mulholland, J.A., Kim, D.H., Takeuchi, M., 2005b. Homologue and isomer patterns of polychlorinated dibenzo-p-dioxins and dibenzofurans from phenol precursors: comparison with municipal waste incinerator data. *Environ. Sci. Technol.* 39, 4398–4406.
- Shadrack, N., 2014. PCDD/PCDF ratio in the precursor formation model over CuO surface. *Environ. Sci. Technol.* 23.
- Sidhu, S.S., Maqsood, L., Dellinger, B., Mascolo, G., 1995. The homogeneous, gas-phase formation of chlorinated and brominated dibenzo-p-dioxin from 2,4,6-trichloro- and 2,4,6-tribromophenols. *Combust. Flame* 100, 11–20.
- Swerev, M., Ballschmiter, K., 1989. Pattern-analysis of pcdds and pcdfs in environmental-samples as an approach to an occurrence source correlation. *Chemosphere* 18, 609–616.
- Syc, M., Fiserova, E., Karban, J., Puncocchar, M., Pekarek, V., 2015. The effect of transient operations on the levels and congener profiles of PCBz, PCPh and PCDD/F in raw flue gases of MSWI plant. *Chemosphere* 118, 261–267.
- Tejima, H., Nishigaki, M., Fujita, Y., Matsumoto, A., Takeda, N., Takaoka, M., 2007. Characteristics of dioxin emissions at startup and shutdown of MSW incinerators. *Chemosphere* 66, 1123–1130.
- Trivedi, J., Majumdar, D., 2013. Memory effect driven emissions of persistent organic pollutants from industrial thermal processes, their implications and management: a review. *J. Environ. Manag.* 119, 111–120.
- Tuppurainen, K., Asikainen, A., Ruokojärvi, P., Ruuskanen, J., 2003. Perspectives on the formation of polychlorinated dibenzo-p-dioxins and dibenzofurans during municipal solid waste (MSW) incineration and other combustion processes. *Acc. Chem. Res.* 36, 652–658.
- Wang, H.C., Hwang, J.F., Chi, K.H., Chang, M.B., 2007a. Formation and removal of PCDD/Fs in a municipal waste incinerator during different operating periods. *Chemosphere* 67, S177–S184.
- Wang, L.C., Hsi, H.C., Chang, J.E., Yang, X.Y., Chang-Chien, G.P., Lee, W.S., 2007b. Influence of start-up on PCDD/F emission of incinerators. *Chemosphere* 67, 1346–1353.
- Weber, R., Hagenmaier, H., 1999. PCDD/PCDF formation in fluidized bed incineration. *Chemosphere* 38, 2643–2654.
- Wehrmeier, A., Lenoir, D., Schramm, K.W., Zimmermann, R., Hahn, K., Henkelmann, B., Kettrup, A., 1998. Patterns of isomers of chlorinated dibenzo-p-dioxins as tool for elucidation of thermal formation mechanisms. *Chemosphere* 36, 2775–2801.
- Xiong, S., Lu, S., Shang, F., Li, X., Yan, J., Cen, K., 2021. Online predicting PCDD/F emission by formation pathway identification clustering and Box-Cox Transformation. *Chemosphere* 274, 129780.
- Yan, J.H., Chen, T., Li, X.D., Zhang, J., Lu, S.Y., Ni, M.J., Cen, K.F., 2006. Evaluation of PCDD/Fs emission from fluidized bed incinerators co-firing MSW with coal in China. *J. Hazard Mater.* 135, 47–51.
- Zhang, M., Buekens, A., Olie, K., Li, X., 2017. PCDD/F-isomers signature - effect of metal chlorides and oxides. *Chemosphere* 184, 559–568.